Fermilab Library
0 1160 0023799 4
ITEP-92-83
35

INSTITUTE OF THEORETICAL AND EXPERIMENTAL PHYSICS

83–92

V.D. Mur, V.S. Popov, Yu.A.Simonov, V.P.Yurov

Description of relativistic heavy-light quark-antiquark systems via Dirac equation

MOSCOW 1992

УДК 530.145 М-16

DESCRIPTION OF RELATIVISTIC HEAVY-LIGHT QUARK-ANTIQUARK SYSTEMS VIA DIRAC EQUATION: Preprint ITEP 92-83/

V.D.Mur, V.S.Popov, Yu.A.Simonov, V.P.Yurov - M., 1992 - 36p.

Starting from the QCD Lagrangian and taking into account both perturbative and nonperturbative effects, we use the method of vacuum correlators to derive the Dirac equation (rigorously for the Coulomb interaction and heuristically for the confining potential) for system consisting of a light quark and heavy antiquark.

As a result the confining potential is a Lorentz scalar, and the Coulomb part — a fourth component of a 4-vector. The energy spectrum of the Dirac equation is considered for zero mass particle interacting via these potentials. Numerical calculations of energy eigenvalues $E = E_{n\kappa}$ and eigenfunctions are performed and some exact solutions of the Dirac equation in the case of $E = m = 0$ are found.

The connection with experimental spectra of D and B mesons is briefly discussed.

Fig. - 7. ref. - 28

© Институт теоретической и экспериментальной физики, 1992

1 Introduction

The quark–antiquark systems consisting of one heavy quark (antiquark) Q and light antiquark (quark) $\bar{q}$ are the QCD analogue of the hydrogen atom and similary to that are of fundamental importance.

Recently the issue of the heavy–light bosons has become a topic of a vivid interest both in the analytic and Monte–Carlo QCD studies [1].

From the theoretical viewpoint the interest of heavy–light systems lies in several aspects. First, in the limit of one infinitely heavy quark mass one hopes to get a dynamics of a light quark in the external field of the heavy one. That would be similar to the picture of the hydrogen atom.

Second, since the exernal field is time–independent, one may hope to obtain a static potential in QCD together with spin-dependent forces, as it was done for heavy quarkonia [2].

An important issue in this connection is the Lorentz nature of the confining part of the potential, arguments in favour of its scalar character are found in the form of inequalities [3], and also in the form of spin–dependent terms [2,4].

Third, in the heavy–light system one may study how the chiral symmetry breaking (CSB) affects the spectrum. When one quark mass is vanishing, in the chiral symmetric case the spectrum would consist of parity doublets, and the CSB lifts the degeneracy.

Forth, using Dirac equation we implement explicity relativistic dynamics and may study relativistic properties of the spectrum, e.g. in the case of vanishing quark mass, and also relativistic spin splittings in the spectrum.

In particular, in our case the spin symmetry widely discussed now [1] is present, since the spin of the heavy quark is decoupled. Hence every state of the Dirac equation with a given j and parity corresponds to two almost degenerate states of the $(q\bar{Q})$ system with $\vec{j}$ and the heavy quark spin $\vec{S} = \frac{\vec{1}}{2}$ adding to $J = j \pm \frac{1}{2}$.

Our final point is that the Dirac equation description yields a dynamical framework for the heavy–light mesons which can be used to calculate meson matrix elements and form factors to compare with experiment and semiphenomenological approaches widely used now in this context [1,5].

Here we attempt to derive explicitly the Dirac equation for the heavy–light quark system starting from the QCD Lagrangian and incorporating both

perturbative and nonperturbative effects in the framework of the Vacuum Correlator Method (VCM) [6-8].

In the course of derivation we use some approximations which are cleary stated at each step, e.g.: neglect of virtual quark pairs (quenching approximation), keeping the lowest (quadratic) cumulant in the cluster expansion and the "limit of local dynamics" [2], $T_g \to 0$, where T_g is the gluonic vacuum correlation length. We discuss physical implications of these approximations in the main text below.

Even with those approximations we are unable to prove rigorously the appearance of the static scalar confining potential, but we give strong arguments in favor of it. The situation is much better for the perturbative part, and the existence of the external vector potential in the limit of one heavy quark mass is explicitly shown.

At this point we start with the Dirac equation containing a vector Coulomb part and a scalar confining part and study properties of its spectrum. For a comparison we have also considered two other cases: i)a vector confining and the Coulomb part; ii) both parts of potential transform as scalars. We are explicitly interesed in the limit of a vanishing light quark mass and spin dependences of the energy eigenvalues.

We show explicitly that reasonable spectrum occurs only for scalar confining part. In this case the scalar potential breaks explicitly chiral symmetry and the states with opposite parities are not degenerate. In the case of vector confining part only quasistationary states have been found.

We have written down possible general symmetry properties of spectral states and in particular cases of zero scalar potential and zero vector potential, and of zero mass.

We also find some exact analytic solutions of the Dirac equation which occur for $E = m = 0$. This enables us to find an equation, defining the value of the Coulomb constant $\zeta = \zeta_{na}$, for which the (nji) discrete energy level reaches the value $E = 0$. We note an analogy of this problem with the relativistic Coulomb problem of an electron in the field of the heavy supercritical nucleus with $Z > 137$ [9-11].

The paper is organized as follows. In Section 2 we use the Feynman–Schwinger representation of the quark–antiquark Green function to derive the limit of one infinitely heavy mass.

In Section 3 we compare this limit with the Dirac equation and discuss the Lorentz nature of the confining interaction.

In Section 4 we discuss the properties of the spectrum of the Dirac equation.

In Section 5 we discuss symmetry properties of the spectrum, in particular chiral properties.

In Section 6 we discuss numerical results for the spectrum of the Dirac equation in the limit of vanishing light quark mass.

In Section 7 we investigate the exact analytic solutions of Dirac equation which occur for $E = m = 0$.

In Section 8 we summarize our results, and compare the Dirac spectrum obtained here with experiment and other approaches. This enables us to discuss also heavy mass corrections.

2 The Feynman–Schwinger representation for the heavy–light Green's function

Consider the quark–antiquark system of one heavy antiquark (with mass m_2) and a light quark of a much smaller mass m_1, which we neglect in some cases below.

The Green's function G of such a system with quarks initially at points $y, \bar{y}$ and finally at points $x, \bar{x}$ is given by the path integral over fermionic and gluonic fields and is written down in Appendix 1. Performing fermionic integrals and neglecting the fermionic determinants (quenching approximation) for simplicity, one arrives at the amplitude, depicted graphically in Fig.1, where Δ_i is the quark Green's function with quark mass m_i, and Γ belong to the initial and final wave-functions:

$$\Psi(y, \bar{y}) = \bar{q}(y)\Gamma(y, \bar{y})q(\bar{y})$$

and analogously for $\bar{\Psi}(x, \bar{x})$. Thus we can write

$$G(x\bar{x} \mid y\bar{y}) = < tr[\Gamma(\bar{x}, x)\Delta_1(x, y)\Gamma(y, \bar{y})\Delta_2(\bar{y}, \bar{x})] > \tag{1}$$

The angular brackets here denote the integration over gluonic fields. This integration we perform using the cluster expansion [6, 7], as discussed in detail in Appendix 1, and we arrive at the following expression involving

proper time and path integrals for quark (s, z) and antiquark $(\bar{s}, \bar{z})$

$$G(xx \mid yy) = \int_0^\infty ds \int_0^\infty d\bar{s} Dz D\bar{z} e^{-K-\bar{K}} \times \tag{2}$$
$$tr[\Gamma_x(m_1 - \hat{D}^{(1)})\gamma_{zz}\Gamma_y(m_2 - \hat{D}^{(2)})],$$

where

$$K = m_1^2 s + \frac{1}{4}\int_0^s \dot{z}^2 d\tau,$$

$$\bar{K} = m_2^2 \bar{s} + \frac{1}{4}\int_0^{\bar{s}} \dot{\bar{z}}^2 d\bar{\tau}$$

In (2) Γ_x, Γ_y refer to the Lorentz structures in initial and final states, $D^{(i)}$ should be expressed as in (A.15) and γ_{zz} is given in (A.14), which we rewrite here in the form (in the lowest order of cluster expansion, where perturbative and nonperturbative contributions factorize [8], see eq.(A.13))

$$\gamma_{zz} = exp\{-\frac{g^2}{2}\int df_{\mu\nu}(z)df_{\rho\lambda}(z') < F_{\mu\nu}(z)F_{\rho\lambda}(z') >\} \tag{3}$$

where

$$df_{\mu\nu}(z) \equiv ds_{\mu\nu}(z) - i\sigma^{(1)}_{\mu\nu}d\tau + i\sigma^{(2)}_{\mu\nu}d\bar{\tau} \tag{4}$$

and $< F\ F >$ is the gluonic correlator which can be split into perturbative and nonperturbative part as in (A.13).

Note, that one should keep the proper ordering of spin indices under the sign of tr in (A.16), e.g. spin indices of $\rho^{(1)}$ in γ_{zz} enter to the left of Γ_y, while those of $\rho^{(2)}$ to the right of Γ_y.

Now we discuss the limit of one heavy mass, $m_2 \to \infty$. In this case, when m_2 is much larger than the interaction strength, the particle 2 is moving along the straight line trajectory

$$\bar{z}_\mu = \bar{y}_\mu + \frac{\bar{x}_\mu - \bar{y}_\mu}{\bar{s}}\bar{\tau}, \quad 0 \le \bar{\tau} \le \bar{s} \tag{5}$$

$$\bar{x}_4 - \bar{y}_4 \equiv T; \quad \frac{T}{\bar{s}} = 2m_2 \ ; d\bar{\tau} = \frac{d\bar{z}_4}{2m_2};$$

$\bar{z}_i = \bar{y}_i = \bar{R}_i$ — position in space of particle 2.

One can see that in this limit the spin interaction of particle 2 (terms $\rho^{(2)} d\bar{\tau}$) is $\sim 0\ (1/m_2)$ and can be neglected.

The perturbative part of the cumulant (A.13) can be written as

$$g^2 \int d\sigma_{\mu\nu}(u) \int d\sigma_{\rho\lambda}(u') \ll F_{\mu\nu}(u) F_{\rho\lambda}(u') \gg_{pert} =$$

$$= g^2 \int_C dz_\mu \int_C dz'_\rho < A_\mu(z) A_\rho(z') >_{pert} = \tag{6}$$

$$= \frac{C_2 g^2}{4\pi^2} \int_C dz_\mu \int_C \frac{dz'_\mu}{(z-z')^2}$$

where C_2 is the quadratic Casimir operator, $C_2(N_C = 3) = \frac{4}{3}$ and C is the closed contour depicted in Fig.1. The integral in (6) is divergent and is regularized by the insertion of the Z factor in front of the exponential in (3) and introducing the *minimal distance* δ of the points z and z' in (6), for details see [14].

Therefore we can now study the situation when only perturbative interaction is present, and the Green's function looks like

$$G(z\bar{z} \mid y\bar{y}) = \int_0^\infty ds Dz e^{-m_1^2 s - \frac{1}{4}\int_0^s \dot{z}^2 d\tau} tr[\Gamma_\mu (m_1 + \frac{1}{2}\dot{z}) \times \tag{7}$$

$$\times Z exp\{-g^2 \int (d\sigma_{\mu\nu}(u) + \frac{1}{i}\sigma^{(1)}_{\mu\nu} d\tau) d\sigma_{\rho\lambda}(u') \ll F_{\mu\nu}(u) F_{\rho\lambda}(u') \gg_{pert}\} \times$$

$$\times \Gamma_\mu (m_2(1-\gamma_4))]$$

where we have neglected terms of selfinteraction of particle 1.

Our goal now is to rewrite the exponent in (7) in the form

$$exp\{ig \int (\bar{A}_\mu(z) dz_\mu + \frac{1}{i}\rho^{(1)}_{\mu\nu} \bar{F}_{\mu\nu} d\tau)\} \tag{8}$$

where we (a similar derivation for QED was done in [15]) have defined following (6)

$$\bar{A}_\mu(z) = ig \int < A_\mu(z) A_\rho(z') > dz'_\rho = \frac{ig}{4\pi^2} \int \frac{dz'_\rho}{(z-z')^2} = \tag{9}$$

$$= \frac{ig}{4\pi} \frac{\delta_{\mu 4}}{|\vec{z} - \vec{R}|} C_2$$

Similarly

$$\bar{F}_{\mu\nu} = \partial_\mu \bar{A}_\nu - \partial_\nu \bar{A}_\mu, \tag{10}$$

One can also check that from the explicit expression for $\ll F\,F \gg_{pert}$, which one obtains from the Feynman gauge propagator (6)

$$< A_\mu(z) A_\nu(z') >_{pert} = \frac{1}{4\pi^2} \frac{\delta_{\mu\nu}}{(z-z')^2} \tag{11}$$

Hence we can write the $q\bar{q}$ Green's function keeping only perturbative interaction as

$$G(z\bar{z} \mid y\bar{y}) = tr[\Gamma_\mu G(z,y) \Gamma_\nu m_2 (1-\gamma_0)] \tag{12}$$

where we have defined

$$G(z,y) = \int ds Dz (m_1 - \hat{D}(\bar{A})) e^{-m_1^2 s - \frac{1}{4}\int_0^s \dot{z}^2 d\tau + ig\int_y^z \bar{A}_\mu dz_\mu + g\int_0^s \sigma_{\mu\nu} \bar{F}_{\mu\nu} d\tau} =$$

$$= < z \mid \int_0^\infty ds (m_1 - \hat{D}(\bar{A})) e^{-s(m^2 - (\hat{D}(\bar{A}))^2)} \mid y > = \tag{13}$$

$$= < z \mid (m_1 + \hat{D}(\bar{A}))^{-1} \mid y >$$

and we observe that $G(z,y)$ satisfies the Dirac equation

$$(m_1 + \hat{D}(\bar{A})) G(z,y) = \delta^{(4)}(z-y) \tag{14}$$

In the next section we shall study the effect of nonperturbative interaction.

3 Confining force and the Dirac equation

We now turn to the nonperturbative interaction, which provides confinement due to the presence of the special (Kronecker) structure in the quadratic cumulant [6]. Neglecting again the selfinteraction of light particle, we have the same form of equation as in (7), but we should add there to $\ll F\,F \gg_{pert}$ also the nonperturbative part $\ll F\,F \gg_{nonpert}$, which can be written as [6]

$$\ll F_{\mu\nu}(u) F_{\rho\lambda}(u') \gg = (\delta_{\mu\rho}\delta_{\nu\lambda} - \delta_{\mu\lambda}\delta_{\nu\rho}) D(u-u') + \tag{15}$$

$$+ \frac{1}{2}[\frac{\partial}{\partial u_\mu}((u-u')_\rho \delta_{\nu\lambda} - (u-u')_\lambda \cdot \delta_{\nu\rho}) + \mu\rho \leftrightarrow \nu\lambda] \cdot D_1(u-u')$$

It was shown [6,7], that only D (and not D_1) yields confinement (the area law of the Wilson loop), and we concentrate first on this term, disregarding also the spin term $\sigma^{(1)}_{\mu\nu}$ in (7). We have

$$\int ds_{\mu\nu}(u)\int ds_{\rho\lambda}(u') \ll F_{\mu\nu}(u)F_{\rho\lambda}(u') \gg \to \int ds_{\mu\nu}(u)ds_{\mu\nu}(u')D(u-u') + ... \tag{16}$$

Using the same arguments, as in [6], one can see that we get the area-law exponent in (7), namely for large area we have

$$exp(-\sigma S_{min}), \sigma = \frac{1}{2}\int\int d^2u D(u) \tag{17}$$

where S_{min} is the minimal area inside the contour formed by the straight-line trajectory of the heavy particle and the path $z(\tau)$ of the light one.

We are now facing a fundamental question: i) whether the term (17) can be associated with a local potential V, acting on particle 1; ii) what are the Lorentz properties of this potential — does it transform as a scalar or as a vector?

To answer the question i) we shall follow the arguments given in [2] and therefore we must turn to the exponential (3), defining the dynamics of the system. The integral in the exponent of (3) is over the surface inside the quark and antiquark trajectories; the characteristic length of these trajectories is T_q, a period of quark orbiting.

Being at some point $z(\tau_0)$ on the trajectory, quark is influenced by the fields and through them by his partner. The radius of nonlocality of the fields is given by the correlation length T_g, defining behaviour of $< F(u)F(u') >$ i.e. by functions $D(\frac{u-u'}{T_g})$, $D_1(\frac{u-u'}{T_g})$.

Therefore the criterion of local dynamics is $T_q \gg T_g$ [2,16]. In the opposite case, $T_q \leq T_g$, the quark "feels" all the fields and also motion of antiquark during all his history. This is the nonlocal dynamics, which can be treated by the QCD sum rules [17]. The lattice calculations yield $T_g \sim 0.2 \div 0.3 fm$ [18], while T_q both for light and heavy quarks is $T_q \geq 1 fm$. Therefore the realistic situation is close to the local dynamics.

Regarding the first point, we shall proceed as in [8, 12], forming the minimal surface via the connection of $\gamma \equiv \frac{\tau}{s} = \frac{\tau}{s} = \frac{t}{T}$, where $t = \bar{z}_4 - \bar{y}_4$.

In this case combining all exponents in (19) and (28) we obtain

$$B = \int_0^T dt(\frac{m_1^2}{2\mu_1} + \frac{\mu_1}{2} + \frac{\mu_1}{2}\dot{r}_a^2(t) + \sigma\int_0^1 d\beta\sqrt{\dot{w}^2\cdot r^2 - (\dot{w}_\mu r_\mu)^2}) \tag{18}$$

where we have defined as in [19,8]

$$w_\mu(t) = z_\mu(t)\beta + \bar{z}_\mu(t)(1-\beta), \quad \dot{w}_\mu = \frac{\partial}{\partial t}w_\mu \tag{19}$$
$$r_\mu(t) = z_\mu(t) - \bar{z}_\mu(t); \quad 2\mu_1 = T/s.$$

Taking into account (5) we have

$$w_i(t) = z_i(t)\cdot\beta + R_i(1-\beta); R_i = const \tag{20}$$
$$w_4(t) = z_4(t)\cdot\beta + (\bar{y}_4 + t)(1-\beta)$$
$$\dot{w}_i(t) = \dot{z}_i(t)\cdot\beta = \dot{r}_i(t)\cdot\beta; \quad \dot{w}_4 = \dot{z}_4(t)\cdot\beta + 1 - \beta$$

Following the same procedure as in [19,8] we obtain from B (considered as an action) the proper-time Hamiltonian, depending on the dynamical mass μ_1—

$$H(\mu_1) = \frac{m_1^2}{2\mu_1} + \frac{\mu_1}{2} + \sigma|\vec{r}| + \frac{1}{2\mu_1}(-\frac{\partial^2}{\partial\vec{r}^2}) \tag{21}$$

The eigenvalue of $H(\mu_1)$ is to be minimized with respect to μ_1, which defines the final value of μ_1.

Thus we see that indeed the nonperturbative correlator $\ll FF \gg_{nonpert}$ yields a potential-type term in the proper-time Hamiltonian; provided T_g is small [2] and the expansion of the square-root term in β is done as in [19], which amounts to ~10% accuracy.

It is more difficult to answer another question — about the Lorentz nature of this potential, since eq.(21) is written in the c.m. system and we do not know how this expression transforms under Lorentz boosts. To get a partial understanding of this point, let us compare how vector and scalar potential enter in the Feynman-Schwinger representation for the Green function of a scalar quark (i.e. neglecting spin term $\sim \rho^{(1)}$ in (19)).

We can write for the scalar case

$$G(x,y) \sim \int ds Dz exp(-\int_0^s V_s(z(\tau))d\tau - m^2 s - \int_0^s \frac{\dot{z}^2}{4}d\tau) \tag{22}$$

while for the vector case we have

$$G(x,y) \sim \int ds Dz exp(-m^2 s - \int_0^s \frac{\dot{z}^2}{4}d\tau + i\int_0^s V_\mu dz_\mu) \tag{23}$$

The main difference lies in the fact, that trajectories of the Z-type depicted in Fig.3 (virtual pair creation) give different contribution in scalar and vector case. For the scalar case the proper time intervals $\Delta\tau$, $\Delta\tau_2$ and $\Delta\tau_3$ are positive and add together to suppress thus the pair creation, while in the vector case $\Delta z_4^{(1)}, \Delta z_4^{(2)}$ and $\Delta z_4^{(3)}$ strongly cancel each other, making pair creation easy. In other words, for the scalar potential all parts of a trajectory add arithmetically, while for the vector one should take a vector sum of all intervals along the trajectory.

Looking at our prototype of the potential, the last term in (18), one can see that in this case one actually adds a scalar quantity σdt (we remind that dt is not the fourth component of vector, but rather the proper time $d\tau$, which is scalar). Thus we seem to be justified in treating the confining force as a scalar and not vector.

There are additional arguments in favour of this conclusion.

First of all, in the nonrelativistic derivation of spin-dependent forces in nonperturbative QCD [2], the sign and magnitude of the spin-orbit term depends on whether the confining potential is chosen as scalar, or as a vector [1]. In the Appenix B we quote the spin-dependent terms obtained in [2], for the case of two nonrelativistic quarks. One can notice the asymptotically dominant contribution coming from V_1', which contains only scalar contribution and yields the negative coefficient of the spin-orbit term $\vec{L}\vec{S}$, characteristic for the Thomas precession.

Results obtained in [2] using the cluster expansion and area law unambiguously predict the spin-orbit force corresponding to the Thomas precession term, which was also introduce previously using the string picture [20]. All that corresponds to the scalar confinement.

Second, there are independent arguments in [3], leading to inequalities, which are satisfied for the scalar confining potential, and not satisfied for vector case. Finally the vector confining potential is believed to cause the Klein paradox [10,11]. In Chapters 4 and 6 we study both scalar and vector confining potential and indeed show analytically and numerically that only in the first case one obtains a physically consistent spectrum, corresponding to confinement while in the second case one has only quasistationaly states. This situation is related to the so-called Klein paradox [10,11]. Thus we give strong arguments in favour of the scalar confining potential. Unfortunately at the moment we are still unable to derive from the Schwinger-Feynman

representation the Dirac equation with the scalar potential, in the way we have done it for perturbative Coulomb interaction.

Therefore in the next Sections we simply postulate the Dirac equation with the confining potential of the scalar type (or vector type- to check its inconsistency).

4 The properties of the spectrum of the Dirac equation

As we have shown in the last Sections, the color Coulomb interaction between quarks is of a vector type, and we have argued that the confining interaction is a scalar. It is instructive, nevertheless, to consider both possibilities of interactions, scalar U and vector V, and study properties of solutions of the Dirac equation in these cases.

Assuming spherical symmetry, we shall look for solutions of the Dirac equation in the form

$$\Psi = r^{-1}\begin{pmatrix} G(r)\Omega_{jlM} \\ iF(r)\Omega_{jl'M} \end{pmatrix} \tag{24}$$

where $l + l' = 2j$, and Ω- spherical spinors [21].

Equations for radial wave functions are

$$\begin{aligned} &\frac{dG}{dr} + \frac{\kappa}{r}G - [E + m + U(r) - V(r)]F = 0, \\ &\frac{dF}{dr} - \frac{\kappa}{r}F + [E - m - U(r) - V(r)]G = 0, \end{aligned} \tag{25}$$

where E and m are the energy and mass of the light particle ($m \equiv m_1$ in the notations of Section 2), $\kappa = -(l+1)$ for the states with $j = l + \frac{1}{2}$, $\kappa = l$ for $j = l - \frac{1}{2}$, so that $|\kappa| = j + \frac{1}{2} = 1, 2, \ldots$ We consider three choices.

a) Assume

$$U(r) = M^2 r, V(r) = -\frac{\zeta}{r}, M^2 \equiv \sigma; \zeta = \frac{4}{3}\alpha_s. \tag{26}$$

Putting $m = 0$ and introducing dimensionless variables: $x \equiv Mr, \varepsilon = E/M$, we arrive at

$$G' + \frac{\kappa}{x}G - (\varepsilon + x + \zeta \cdot x^{-1})F = 0, \tag{27}$$

$$F' - \frac{\kappa}{x}F + (\epsilon - x + \zeta \cdot x^{-1})G = 0.$$

(hereafter the prime denotes the derivative in x).

Let us find the asymptotics of radial functions at zero and infinity. For $x \to 0$, inserting the expansions $G = Ax^{\nu} + ..., F = Bx^{\nu} + ...$ into (27), we obtain

$$\nu = (\kappa^2 - \zeta^2)^{1/2}, A/B = \kappa^{-1}(\kappa^2 - \zeta^2)^{1/2} - 1 \qquad (28)$$

The wave function is regular at zero for $\zeta <| \kappa |= j + \frac{1}{2}$, while for $\zeta > j + \frac{1}{2}$ there occurs a well known in quantum mechanics "collapse to the center" [22,23]. The difficulty is actually of a formal character and can be removed introducing a cut-off of the Coulomb potential at small distances, $r < r_0$ – in the same way as in QED with the charge $Z > \alpha^{-1} = 137$, see refs. [9-11, 24,25].

The behaviour of wave functions at infinity is more complicated. From (27) it follows that $G, F \sim exp(\pm\frac{1}{2}x^2)$ as $x \to \infty$, and the solution with a positive exponent is clearly not admissible.

We accordingly write G, F as

$$G \approx A' exp\{-(ax^2 + bx)\}x^{\beta}(1 - \frac{c_1}{x} + ...), \qquad (29)$$

$$F \approx B' exp\{-(ax^2 + bx)\}x^{\beta}(1 - \frac{c_1'}{x} + ...).$$

Inserting these expansions into (27) we find after elementary (however tedious) calculations

$$A' = -B', a = 1/2, b = 0, \beta = \frac{1}{2}\epsilon^2, c_1 = (\zeta - 1/2)\epsilon, c_1' = (\zeta + \frac{1}{2})\epsilon, ... \qquad (30)$$

Thus the wave functions (w.f.) fall off at infinity mostly in the same way as in the case of harmonic oscillator in nonrelativistic quantum mechanics. The solution satisfying the conditions obtained above, (28) and (29), exists only for some definite values of $\epsilon = \epsilon_n(\zeta, \kappa)$, and the w.f. is normalizable. Therefore for the Dirac equation only the discrete spectrum exists.

This conclusion holds for any scalar potential which grows at infinity,

$$G(r), F(r) \sim exp(-\int_0^r U(r')dr'), r \to \infty \qquad (31)$$

Even for the logarithmic potential the w.f. decrease asymptotically faster than exponentially:

$$G, F_{(r\to\infty)} \sim exp(-g r \ln r) \quad \text{for} \quad U(r) = g \ln r \qquad (32)$$

b) When both interactions are of a vector type, i.e.

$$U(r) = 0, V(r) = -\zeta r^{-1} + M^2 r, \qquad (33)$$

the system of radial equations is

$$G' + \frac{\kappa}{x}G - (\epsilon + \frac{\zeta}{x} - x)F = 0, \qquad (34)$$

$$F' - \frac{\kappa}{x}F + (\epsilon + \frac{\zeta}{x} - x)G = 0.$$

In this case at $x \to 0$

$$\nu = (\kappa^2 - \zeta^2)^{1/2}, A/B = \kappa/[\kappa + (\kappa^2 - \zeta^2)^{1/2}],$$

while the parameters in the eq.(29) assume the values

$$A' = iB', a = -i/2, b = i\epsilon, \beta = -i\zeta$$

Here we chose a solution satisfying the Sommerfeld radiation condition, i.e. having an outgoing wave at $r \to \infty$. Thus for the interaction (33) the discrete spectrum is absent (see also the curve b in Fig.4) and all solutions of the Dirac equation, if any, are quasistationary. In the special case of the rectangular well one can obtain an exact analytic equation for the spectrum [26]. The width of these quasistationary states defines the probability of the spontaneous pair creation in the potential (33). This phenomenon is closely connected with the so-called Klein paradox [10,11]. Physically it means that the problem is now of many-particle type, but actually the Dirac equation is still applicable.

c) Consider for completeness also the case of purely scalar interactions,

$$U = -\zeta r^{-1} + M^2 r, \quad V = 0. \qquad (35)$$

In this case we have at $r \to 0$ instead of (28)

$$\nu = (\kappa^2 + \zeta^2)^{1/2}, A/B = [\kappa - (\kappa^2 + \zeta^2)^{1/2}]/\zeta \qquad (36)$$

Thus the "collapse to the center" does not occurs for arbitrary large values of the Coulomb parameter ζ. At infinity we obtain the behaviour which is analogous to (29): $G, F \sim exp(-\frac{1}{2}M^2r^2)$, therefore the spectrum is discrete.

Hence the character of the energy spectrum depends crucially on the assumption about the nature of the confining interaction M^2r (scalar or vector).

The reason can be understood qualitatively using the method of the effective potential [25,27].

The system (25) corresponds in the quasiclassical approximation (neglecting spin–orbit and spin–spin forces) to the following relation between energy and momentum

$$p^2(r) = (E - V(r))^2 - (m + U(r))^2 + \kappa^2 r^{-2} \equiv 2m(\tilde{E} - U_{eff}), \qquad (37)$$

where $\tilde{E}$ and U_{eff} are effective energy and potential in the nonrelativistic Schrödinger equation:

$$\tilde{E} = \frac{1}{2m}(E^2 - m^2), \quad U_{eff} = \frac{1}{2m}(U^2 - V^2) + U + \frac{\kappa^2}{2mr^2} \qquad (38)$$

In the nonrelativistic limit ($E \approx m$ and $U, | V | \ll m$) we have: $U_{eff} \approx U + V + (l + 1/2)^2/2mr^2$. Therefore, all three cases $(a) - (c)$ correspond the funnel potential $V_{NR}(r) = -\zeta/r^{-1} + \sigma r$, which is often used in QCD.

However for large U and V, the situation is drastically different for our cases a) - c). This can be understood from Fig. 4, where the qualitative behaviour of $U_{eff}(r)$ is shown.

5 Symmetry properties of the spectrum of the Dirac equation

Here we discuss symmetries of solutions of the Dirac equation for particles of zero mass.

It is clear that in case when both m and U are zero the Dirac equation (and the corresponding term in the Lagrangian) are chirally symmetric, i.e. do not charge under a global transformation:

$$\Psi \to e^{i\alpha\gamma_5}\Psi \quad , \bar{\Psi} \to \bar{\Psi}e^{i\alpha\gamma_5} \qquad (39)$$

From the point of view of the spectrum the chiral symetry means that all states are parity degenerate, i.e. masses of the states 0^+ and 0^- (or 1^+ and 1^-) are the same.

It is easy to demonstrate that the system (25) with $m = 0$ is invariant under even more general transformation when $U \neq 0$:

$$E \to E, \kappa \to -\kappa, U \to -U, V \to V, \qquad (40)$$
$$G(r) \to -F(r), F(r) \to G(r).$$

It follows from (40) that for $U \equiv 0$ the spectrum is degenerated with respect to the sign of the Dirac quantum number κ, i.e. it depends only on the total momentum j, and not on the way l and s are coupled (the chiral degeneracy).

Another symmetry of the Dirac equation is

$$E \to -E, \kappa \to -\kappa, U \to U, V \to -V, \qquad (41)$$
$$G(r) \leftrightarrow F(r),$$

which in contrast to (40) connects the states with positive and negative energy. In particular, for $V \equiv 0$ (scalar interaction) there is a doubling of states with a given $| E_n |, E_n = \pm | E_n |$, and we can always consider $E_n > 0$. In the specific case $E = 0$ (zero modes) there is , at the first sight, a chiral degeneracy of states. However, it is easy to show that the degenerate states with $\varepsilon = 0$ do not exist at all. Indeed, multiplying the first eq.(25) by G, the second — by F and integrating the difference from $r = 0$ to $r = \infty$, we obtain an identity:

$$\int_0^\infty (G^2 + F^2)\frac{dr}{r} = 2\kappa^{-1}\int_0^\infty (E - V)GFdr \qquad (42)$$

(we have used in the derivation that G and F vanish both at $r = 0$ and $r = \infty$). From eq.(42) one can see for the purely scalar interaction, the absence of solutions with zero energy.

6 Results of numerical calculations

Here we report our results of numerical calculations. In Fig.5 is shown the dependence of eigenvalues $\varepsilon_{n\kappa} = E_{n\kappa}/M$ on the ratio $\zeta/ | \kappa |$ for the potential

(26) (solid lines correspond to the lowest states of a given value of κ, $n = 1$; the dashed lines are for the first excited states, $n = 2$). The energy eigenvalues decrease monotonically with the growing Coulomb parameter ζ, and for $\zeta \to |\kappa|$ they have a square-root-type singularity. The latter is characteristic for the potentials with the Coulombic behaviour at $r \to 0$ and is connected to the phenomenon of "the collapse to the center" [10,11].

In Fig.5 one can see that the levels with $\kappa > 0$ lie much higher than those with $\kappa < 0$ (for a given n). The physical meaning of this effect becomes clear, when one remembers that the centrifugal barrier is proportional to $\kappa(\kappa+1)$ and e.g. is absent for $\kappa = -1$ in contrast to the case of $\kappa = +1$. The energy of the levels are also listed in the Table for several lowest levels.

We note, that the singularity at $\zeta = |\kappa|$ can be removed when one introduces a cut-off of the Coulomb potential $V(r) = -\zeta/r$ at small distances:[1]

$$V(r) = \begin{cases} -\zeta r^{-1}, r > r_0 \\ -\frac{\zeta}{r_0} f(r/r_0), 0 < r < r_0 \end{cases} \tag{43}$$

where r_0 is the cut-off-radius and $f(0) < \infty$.

In case of $r_0 \ll M^{-1}$ the influence of the cut-off on the energy levels is essential only in the nearest vicinity of the point $\zeta = |\kappa|$. Here the level sinks to the boundary $\varepsilon = 0$ (it corresponds to a boundary $\varepsilon = -m$ for $m \neq 0$) at some value $\zeta = \zeta_{cr} > |\kappa|$, which depends both on r_0 and on the concrete form of the cut-off function $f(r/r_0)$ in eq.(43).

With the further increase of ζ the level goes on down to the region of negative values of energy, but the spectrum stays discrete (this is in contrast to the Coulombic problem with the vector potential [10,11]), which means that the pair creation does not take place.

7 Exact solutions for $E = 0$

In QED the solutions of the Dirac equation simplify considerably for $E = \pm m$, which corresponds in our case ($m = 0$) to $E = 0$. Eqs. (27) in terms of linear combinations $u = G + F, v = G - F$ assume the form ($\varepsilon = 0$)

[1] In case of the lowest levels with $\kappa < 0$, for which $\varepsilon(\kappa) \to 0$ in the limit $\zeta \to |\kappa|$ (see Fig.5), this singularity can be derived analytically — see below eq. (46).

$$u' - xu + \frac{\kappa+\zeta}{x} v = 0, \quad v' + xv + \frac{\kappa-\zeta}{x} u = 0 \tag{44}$$

At $\zeta = -\kappa$ the first equation can be solved explicitly, $u = C exp(\frac{x^2}{2})$, which yields $C = 0$ and hence $G = -F = \frac{1}{2}v$. The normalized wave functions are [2]

$$G(x) = -F(x) = \pi^{-1/4} exp(-x^2/2) \tag{45}$$

Using the perturbation theory in the parameter $(\kappa^2 - \zeta^2)^{1/2} \ll 1$, one can define the behavior of the energy near $\zeta = -\kappa$:

$$\varepsilon(\zeta) = \pi^{-1/2}(1 - \zeta^2/\kappa^2)^{1/2} + ... \tag{46}$$

(for details see Appendix C). Computations confirm this asymptotic expansion — see Fig.6.

Note, that the solution of the type (45) exists only for the states with $\kappa < 0$. In case when $\zeta = \kappa$ the equations (44) have a nonzero solution $G = F = const \cdot exp(x^2/2)$ which is not admissible because of the exponential growth at infinity.

These results can be generalized to arbitrary values of ζ and κ. Solving in (44) for one of functions u, v, we come to the equation

$$w'' + \frac{1}{x} w' - [\pm 2 + x^2 + \frac{\kappa^2 - \zeta^2}{x^2}] w = 0, \tag{47}$$

where the upper (lower) sign corresponds to the function $u(v)$. We shall consider the case $\zeta > |\kappa|$, when the cut-off of the Coulomb part of the potential is essential. Solution of these equations for $r > r_0$, decreasing at infitity, can be expressed through the Whittaker functions [28],

$$u = C_1 x^{-1} W_{-1/2, ig}(x^2), \quad v = C_2 x^{-1} W_{1/2, ig}(x^2), \tag{48}$$

where $g = (\zeta^2 - \kappa^2)^{1/2} > 0$, and C_1, C_2 are some constants.

Insertion of (48) into the first of eqs (44) yields the connection between C_1, C_2:

$$C_1 = 2(\kappa + \zeta) C_2 \tag{49}$$

[2] This result can be easily generalised to the case $m \neq 0$ and arbitrary scalar potential $U(r)$.

In the internal region, $0 < r < r_0$, the Dirac equation should be solved with the cut-off potential (43), where one can neglect linear potential because $r_0 \ll 1/M$. For the simplest case $f(x) \equiv 1$ (a square-well type cut-off) the solution is found analytically and can be expressed through the Bessel functions with half-integer index.

The energy spectrum is found from the matching of the internal and external solutions at $r = r_0$. In case of the Dirac equation one can match the ratio F/G instead of logarithmic derivative.

As a result we have

$$2(\kappa + \zeta)W_{-1/2,i\varrho}(x_0^2)/W_{1/2,i\varrho}(x_0^2) = \xi, \tag{50}$$

where $\xi = u(x_0)/v(x_0)$ is defined from the internal solution and depends on κ, ζ and the cut-off model. E.g. for the states with $\kappa = \mp 1$ in the square-well-cut-off case we have

$$\xi(\kappa = -1) = -1/\xi(\kappa = 1) = \frac{1 - \zeta(1 + ctg\zeta)}{1 + \zeta(1 - ctg\zeta)} \tag{51}$$

The equation (50) can be solved numerically and it defines the dependence of the Coulomb constant ζ_{nm}, for the n-th level sinking to the boundary $\varepsilon = 0$, on the cut-off radius r_0 (for a certain choice of the cut-off function $f(x)$).

8 Discussion and conclusions

In conclusion we discuss the structure of the resulting spectrum, briefly compare it to the experiment and summarize our results.

We start with the nonrelativistic spectrum and use the formulas, given in Appendix B, which yield the spectrum shown in Fig. 7a. Here the splitting between the $S = 1$ and $S = 0 (L = 0)$ levels is due to the hyperfine interaction and, as is seen in Appendix B, is proportional to $(m_1 m_2)^{-1}$. When both masses are large ($m_i \gg M = \sigma^{1/2}$), all splittings are small including spin-spin ($0((m_1 m_2)^{-1})$ and spin-orbit, which contains terms $0(m_1^{-2})$, $0(m_2^{-2})$ and $0((m_1 m_2)^{-1})$ which one can denote as $(LS)_1$, $(LS)_2$ and $(LS)_{12}$ — see Appendix B.

In the case when $m_2 \gg m_1 \sim M$, Fig.7b, the intervals of $(LS)_1$ become the largest and the spectrum transforms in such a way, that the coupling of

the spin of particle 2 becomes very weak and in the limit $m_2 \to \infty$ it finally decouples, which results in the Wise–Isgur symmetry [5]. Namely, the states can be classified by the total momentum of the light particle j, while the states of total momentum of the system $\vec{J} = \vec{j} + \vec{S}_2$ are degenerated with respect to the direction of $\vec{S}_2$.

This is what one observes in the Dirac spectrum, see Fig. 5 of our numerical calculations, and Fig. 7c, giving a schematic description of the Dirac spectrum. Here the degeneration (Isgur–Wise symmetry) is complete.

This should be compared to the experimental picture Fig. 7d, where for the charmed mesons the order of the levels is the same as in Figs. 7b, 7c, but the splittings are still large. For B-mesons the splitting of lowest levels is 3 times less (52 MeV) as it should be, since the mass of the c quark is ≈ 3 times smaller than that of b quark. We also note, that the experimental splitting $\Delta E \sim 450 MeV$ between $j = \frac{1}{2}$ and $j = \frac{3}{2}$ states, is reproducible in our results, when one takes $\sqrt{\sigma} \sim 0.5 GeV$ and $\zeta \sim 0.6 \div 0.8$.

Thus we can conclude, that the Dirac equation yields a reasonable qualitative description of the realistic spectrum. We hope to discuss this point in more detail in future publications, where we also give predictions for the D_S, B and B_S mesons.

Summarizing our results, we have derived the Dirac equation from the Feynman-Schwinger representation of the quark-antiquark Green's function in case of the colour Coulomb interaction.

Assuming that the confining interaction can be introduced into the Dirac equation similarly to the Coulomb interaction, we have clarified the Lorentz structure of the confining interaction connecting a light quark to a heavy antiquark.

The analysis of the solutions of the Dirac equation shows that the growing at infinity potential yields confinement only if it is the scalar and not the time component of the 4-vector. In this aspect there is an essential difference from the nonrelativistic case.

We have also studied the dependence of the charge ζ in the critical region, $\zeta \sim |\kappa|$, and found its dependence on the cut-off of the Coulomb potential. We have computed energy eigenvalues for several lowest levels and have compared it with nonrelativistic spectrum and experimental results.

Appendix A

The Feynman–Swinger representation of the quark–antiquark Green's function.

The probability amplitude of quark and antiquark initially at points $y, \bar{y}$ in the state $\Psi(y,\bar{y}) = \bar{\Psi}(y)\Gamma(y,\bar{y})\Psi(\bar{y})$ to reach the points $x, \bar{x}$ in the state $\Psi(x,\bar{x}) = \bar{\Psi}(x)\Gamma(x,\bar{x})\Psi(\bar{x})$ is given by the path integral in the Euclidean space–time

$$G(x\bar{x} \mid y\bar{y}) = \frac{1}{N}\int DA_\mu D\Psi D\Psi^+ \quad \Psi^+(x,\bar{x})\Psi(y,\bar{y})e^{-S}, \qquad (A.1)$$

where we have omitted for simplicity gauge–fixing and Faddeev–Popov terms, N is the normalization factor and the Euclidean action is

$$S = \int d^4x[tr\frac{1}{4}F^2_{\mu\nu} + \Psi^+_1(\hat{D}_1 + m_1)\Psi_1 + \Psi^+_2(\hat{D}_2 + m_2)\Psi_2] \qquad (A.2)$$

Performing the fermionic part of path integration we obtain

$$G(x\bar{x} \mid y\bar{y}) = \int DAe^{-S_0(A)}det(\hat{D}_1 + m_1)\cdot det(\hat{D}_2 + m_2)(\prod_1 - \prod_2) \qquad (A.3)$$

where

$$\prod_1(x\bar{x} \mid y\bar{y}) = tr\Gamma(\bar{x}x)\Delta_1(x\bar{x})tr\Gamma(y,\bar{y})\Delta_2(\bar{y}y), \qquad (A.4)$$

$$\prod_2(x\bar{x} \mid y\bar{y}) = tr\Gamma(\bar{x}x)\Delta_1(x,y)\Gamma(y,\bar{y})\Delta_2(\bar{y},\bar{x}), \qquad (A.5)$$

and $\Delta_i(x,y) = < x \mid (D + m_i)^{-1} \mid y >$.

Note that $\prod_1$ is nonzero only for $m_1 = m_2$ and in the singlet flavour channel. $\prod_1$ corresponds to the disconnected quark–line diagram Fig. 2, which describes the OZI– forbidden processes, while $\prod_2$ contains one quark contour in Fig. 1, and describes the OZI allowed processes.

All terms in (3), i.e. $det_1, det_2, \prod_1, \prod_2$ should be regularized, and we shall discuss this procedure explicity below.

The determinants in (3) correspond to additional quark loops; this contribution is suppressed in the limit of large N_c and neglect of it (the so-called quaenching approximation) seems to be a reasonable approximation

in Monte Carlo simulations. Therefore in what follows we disregard the determinants in (3).

Now we are interested in the case when m_1 and M_2 are different (and moreover, $m_2 \to \infty$ while m_1 is fixed or vanishing). In this case $\prod_1$ vanishes and we are left with the $\prod_2$ averaged over gluonic fields, as in (3)

$$G(x\bar{x} \mid y\bar{y}) = < \prod_2(x\bar{x} \mid y\bar{y}) >_A \qquad (A.6)$$

We now turn to the quark propagator $\Delta(x,y)$ and use for that the Feynman-Schwinger representation [11]

$$\Delta(x,y) = (m - \hat{D})\int_0^\infty dse^{-(m^2-\hat{D}^2)s} = \qquad (A.7)$$
$$(m - \hat{D})\int_0^\infty dsDxe^{-m^2s-\frac{1}{4}\int_0^s \dot{x}^2(\tau)d\tau}\gamma_x(x,y \mid A)$$

where s sometimes is called the proper–time, however this name should be rather given to the parameter τ in the exponent of (A.7).

$$\gamma_x(x,y \mid A) = \Phi(x,y)Pexp\{\int_0^s d\sigma \cdot f(z(\sigma),y)\}, \qquad (A.8)$$

$$f(z,y) = \Phi(y,z)g\Sigma F(z)\cdot\Phi(z,y); \quad \Phi(x,y) = Pexp\{ig\int_y^x A_\mu dz_\mu\} \qquad (A.9)$$

Note that the phase integrals Φ are taken always along the quark trajectory $z(\tau)$.

We have denoted as in [2]

$$g\sigma F(z) = g\begin{bmatrix} \vec{\sigma}\vec{B}(z), & \vec{\sigma}\vec{E}(z), \\ \vec{\sigma}\vec{B}(z), & \vec{\sigma}\vec{E}(z), \end{bmatrix} \qquad (A.10)$$

and $\vec{E}, \vec{B}$ are color–electric and color–magnetic fields.

We now take into account that $\Gamma(x,\bar{x})$ (and analogously $\Gamma(y,\bar{y})$) contains the phase factor $\Phi(x\bar{x})$ along a fixed contour and therefore $\prod_2$ contains an integral Φ over a closed contour, depicted in Fig.1. Spin interactions have the form of insertions of $g\Sigma F$ at some points of the contour. Also the projectors $(m_i - \hat{D}_i)$ appear at the final (or initial) points $x, \bar{x}$ as additional insertions in the contour. Without these insertions (neglecting spins of quarks) one

obtains that the $q\bar{q}$ Green's function is proportional to an average of the Wilson loop:

$$G_s(x\bar{x} \mid y\bar{y}) \sim < W(C) >_A \equiv < \frac{1}{N_c} tr P exp\{ig \int_C dz_\mu A_\mu\} >_A \qquad (A.11)$$

where the contour C is depicted in Fig.3.

We can use for $< W >$ the cluster expansion [6-8]

$$< W(C) >= exp \sum_{m=1}^{\infty} \frac{(ig)^m}{m!} \int d\sigma(1)...d\sigma(m) \ll F(1)...F(m) \gg \qquad (A.12)$$

where the integration is over the minimal surface inside the contour C, and $\ll F(1)...F(m) \gg$ are the cumulants of the order m. For simplicity we shall keep only the lowest cumulant, $m = 2$ and take into account, that in this approximation perturbative and nonperturbative coontributions enter additively [8].

$$\ll F(x)F(y) \gg \equiv \frac{tr}{N_c} < F(x)\Phi(x,y)F(y)\Phi(y,x) >= \qquad (A.13)$$
$$= \ll F(x)F(y) \gg_{pert} + \ll F(x)F(y) \gg_{nonpert}$$

Now one can take into account spin degrees of freedom in the terms γ_s, eqs(7,8) using the formula from [12,13] and keeping again only quadratic cumulant

$$\gamma_{sz} \equiv < \frac{1}{N_c} tr \gamma_s(x,y \mid A)\Phi(y,\bar{y})\gamma_z(\bar{y},\bar{x} \mid A)\Phi(\bar{x},x) >_A = \qquad (A.14)$$
$$= exp\{-\frac{g^2}{2} \int [ds_{\mu\nu}(u) + \frac{1}{i}\sigma^{(1)}_{\mu\nu} d\tau - \frac{1}{i}\sigma^{(2)}_{\mu\nu} d\bar{\tau}] \times$$
$$\times [ds_{\rho\lambda}(u') + \frac{1}{i}\sigma^{(1)}_{\rho\lambda} d\bar{\tau}] \ll F_{\mu\nu}(u)F_{\rho\lambda}(u') \gg \}$$

where $\sigma_{\mu\nu} = -\frac{i}{4}(\gamma_\mu\gamma_\nu - \gamma_\nu\gamma_\mu)$, and the superscript i referes to spin variables of the i-th particle.

Finally, we must include in (14) also factors $(m_i - \hat{D}_i)$. Using [12] one has the correspondence

$$D_\mu(x) \to -\frac{1}{2}\dot{x}_\mu(\tau) \qquad (A.15)$$

where $\dot{x}_\mu$ is the derivative in τ of the coordinate on the path. Assembling all terms together in (5-6) we obtain:

$$G(x\bar{x}, \mid y\bar{y}) = \int_0^\infty ds \int_0^\infty d\bar{s} D_z D\bar{z} e^{-m_1^2 s - m_2^2 \bar{s} - \frac{1}{4}\int_0^s \dot{z}^2 d\tau - \frac{1}{4}\int_0^{\bar{s}} \dot{\bar{z}}^2 d\bar{\tau}} \times \qquad (A.16)$$
$$\times tr[\Gamma_x(m_1 + \frac{1}{2}\hat{\dot{z}})\gamma_{sz}\Gamma_y(m_2 + \frac{1}{2}\hat{\dot{\bar{z}}})]$$

In (A.16) Γ_x and Γ_y refer to the Lorentz structures in initial and final states, $\Gamma(x\bar{x})$ and $\Gamma(y\bar{y})$, e.g. for the pseudoscalar channel $\Gamma_x = \Gamma_y = \gamma_5$.

Appendix B

The nonrelativistic spectrum of two particles with all spin interactions taken into account can be obtained in the perturbative way ($1/m$ expansion).

$$m = m_1 + m_2 + E(n) + < n \mid \left(\frac{\vec{\sigma}_1\vec{L}}{m_1^2} + \frac{\vec{\sigma}_2\vec{L}}{m_2^2}\right)\left(\frac{1}{4r}\frac{d\varepsilon}{dr} + \frac{1}{2r}\frac{dV_1}{dr}\right) \qquad (B.1)$$

$$+\frac{(\vec{\sigma}_1+\vec{\sigma}_2)\vec{L}}{2m_1m_2}\frac{1}{r}\frac{dV_2}{dr} + \frac{\vec{\sigma}_1\vec{\sigma}_2}{12m_1m_2}V_4(r) +$$

$$+\frac{1}{12m_1m_2}(3\vec{\sigma}_1\vec{n}\cdot\vec{\sigma}_2\vec{n} - \vec{\sigma}_1\vec{\sigma}_2)V_3(r) \mid n >$$

Contributions of the scalar interaction $U(r) = \sigma r$ and the vector interaction $V(r) = -\frac{4\alpha_s}{3r}$ into the spin splittings are

$$\frac{1}{r}\frac{d\varepsilon}{dr} = \frac{\sigma}{r} + \frac{4}{3}\frac{\alpha_s}{r^3}; \quad \frac{1}{r}V_1' = -\frac{\sigma}{r}; \quad \frac{1}{r}V_2' = \frac{4}{3}\frac{\alpha_s}{r^3};$$

$$V_4 = \frac{32\pi\alpha_s}{3}\delta^{(3)}(\vec{r}), \quad V_3 = \frac{4\alpha_s}{r^3} \qquad (B.2)$$

The main difference appears in V_1' where only scalar interaction enters. Note that the overall sign of spin-orbit terms due to the scalar (σr) and vector ($-\frac{4}{3}\alpha_s/r$) potentials is different.

Appendix C

Let us study the behaviour of energy levels with $n = 1$ and $\kappa < 0$ in the limit $\zeta \to -\kappa$.

Assuming

$$\mu = (1 - \zeta^2/\kappa^2)^{1/2} \to 0, \quad \epsilon = c\mu + 0(\mu^2), \qquad (C.1)$$

$$G = exp(-x^2/2)[1 + \mu g(x) + ...], \quad F = -exp(-x^2/2)[1 + \mu f(x) + ...]$$

after insertion into (27) we obtain

$$g' = (x - \kappa x^{-1})(g - f) - c, f' = (x + \kappa x^{-1})(f - g) + c \qquad (C.2)$$

From(28) it follows that for $x \to 0$

$$g = -\kappa ln x + 1/2 + ..., f = -(\kappa ln x + 1/2 + ...) \qquad (C.3)$$

where omitted are the terms vanising at $x = 0$. Solving eqs.(C.2) with initial conditions (C.3), we get

$$c = \pi^{-1/2}, \quad g = \frac{1}{2}(k - \kappa h), \quad f = -\frac{1}{2}(k + \kappa h), \qquad (C.4)$$

where

$$k(x) = \pi^{-1/2}x \cdot \int_0^\infty e^{-x^2t}(1+t)^{-1/2}dt = \pi^{-1/2}exp(x^2)\Gamma(1/2, x^2), \qquad (C.5)$$

$$h(x) = 2\int_x^\infty k(y)y^{-1}dy$$

and $\Gamma(\alpha, z)$ is the incomplete gamma function [28]. These functions fall off when $x \to \infty$,

$$k(x) = \pi^{-1/2}x^{-1} + 0(x^{-3}), \quad h(x) = 2\pi^{-1/2}x^{-1} + 0(x^{-3}),$$

and for $x \to 0$

$$k = 1 - 2\pi^{-1/2}x + ..., \quad h = 2lnx - 4\pi^{-1/2}x + ...$$

From (C.4) directly follows eq.(46).

Note that

$$\rho \equiv \int_0^\infty G^2 dr / \int_0^\infty F^2 dr = 1 - 4\pi^{-1/2}\mu \int_0^\infty e^{-x^2} k(x) dx + \ldots =$$

$$= 1 - \frac{4}{\pi}\mu + 0(\mu^2) \qquad \text{(C.6)}$$

The fact that ρ is close to unity tells us that for energy $\varepsilon \approx 0$ the motion of the particle is essentially relativistic. The expansions(46) and(C.6) help to check numerical calculations for the values of ζ close to $-\kappa$.

If $\zeta = \pm\kappa$, we have: $g = 0$ in eq. (48) and [28]

$$W_{\pm 1/2,0}(z) = e^{-z/2} z^{1/2} \phi_\pm(z), \qquad \text{(C.7)}$$

where $\phi_+(z) \equiv 1$,

$$\phi_-(z) = z^{-1} \int_0^\infty e^{-t}(1 + \frac{t}{z})^{-1} dt = e^z \Gamma(0, z)$$

If $\zeta = -\kappa$, then $C_1 = 0$, see eq.(49), and $G = -F$ reduce to the elementary functions (45). On the other hand, at $\zeta = \kappa$ the functions $G(x), F(x) \to \infty$ at $x \to 0$, due to the presence of $W_{-1/2,0}$. So, the Dirac equation in this case has no physically admissible solutions with zero energy.

The results obtained above are easily generalized to the case when $V(r) = -\zeta/r$ and the scalar potential U (of an arbitrary form) grows at infinity. For example, we have

$$\varepsilon = c\mu + \ldots, \qquad c = \{2 \int_0^\infty exp[-2 \int_0^r U(r') dr'] dr\}^{-1} \qquad \text{(C.8)}$$

E.g. for $U(r) = gr^N$

$$c = (\frac{g}{2N+2})^{\frac{1}{N+1}} / \Gamma(\frac{N+2}{N+1}), \qquad \text{(C.9)}$$

For $N = 1$ and $g = 1$ eq.(C.9) yields the previously obtained value (C.4).

Table

ζ	κ=-1 n=0	κ=-2 n=0	κ=-3 n=0	κ=1 n=0	κ=2 n=0	κ=-1 n=1
.00000	1.61944	2.14652	2.56927	2.29403	2.70440	2.60263
.05000	1.56569	2.10995	2.53977	2.25085	2.67234	2.55970
.10000	1.51089	2.07305	2.51009	2.20663	2.63992	2.51585
.15000	1.45497	2.03579	2.48022	2.16128	2.60714	2.47102
.20000	1.39787	1.99816	2.45017	2.11470	2.57397	2.42511
.25000	1.33949	1.96017	2.41992	2.06677	2.54040	2.37802
.30000	1.27974	1.92179	2.38948	2.01734	2.50642	2.32963
.35000	1.21850	1.88301	2.35884	1.96626	2.47201	2.27980
.40000	1.15563	1.84382	2.32800	1.91332	2.43714	2.22837
.45000	1.09098	1.80421	2.29695	1.85829	2.40180	2.17512
.50000	1.02434	1.76415	2.26568	1.80085	2.36597	2.11981
.55000	.95548	1.72364	2.23420	1.74064	2.32962	2.06211
.60000	.88407	1.68266	2.20251	1.67717	2.29273	2.00161
.65000	.80971	1.64118	2.17058	1.60979	2.25526	1.93778
.70000	.73187	1.59919	2.13842	1.53759	2.21718	1.86984
.75000	.64976	1.55666	2.10603	1.45930	2.17847	1.79673
.80000	.56223	1.51357	2.07339	1.37292	2.13907	1.71676
.85000	.46736	1.46990	2.04050	1.27508	2.09896	1.62712
.90000	.36154	1.42560	2.00736	1.15918	2.05808	1.52224
.95000	.23570	1.38066	1.97396	1.00811	2.01639	1.38773
.97000	.17354	1.36249	1.96052	.92573	1.99947	1.31539
.98000	.13684	1.35337	1.95378	.87366	1.99096	1.27001
.99000	.09209	1.34421	1.94704	.80561	1.98241	1.21107
1.00000	.00000	1.33503	1.94028	.64007	1.97382	1.06895

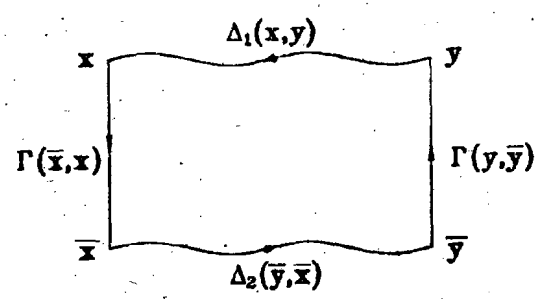
$\Delta_1(x,y)$
x
y
$\Gamma(\bar{x},x)$
$\Gamma(y,\bar{y})$
$\bar{x}$
$\bar{y}$
$\Delta_2(\bar{y},\bar{x})$

Fig. 1

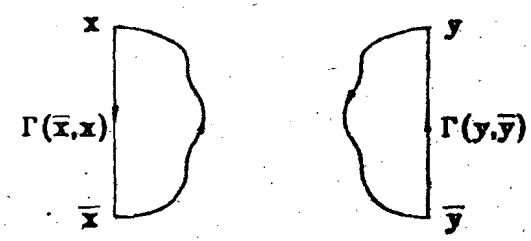
x
$\Gamma(\bar{x},x)$
$\bar{x}$
y
$\Gamma(y,\bar{y})$
$\bar{y}$

Fig. 2

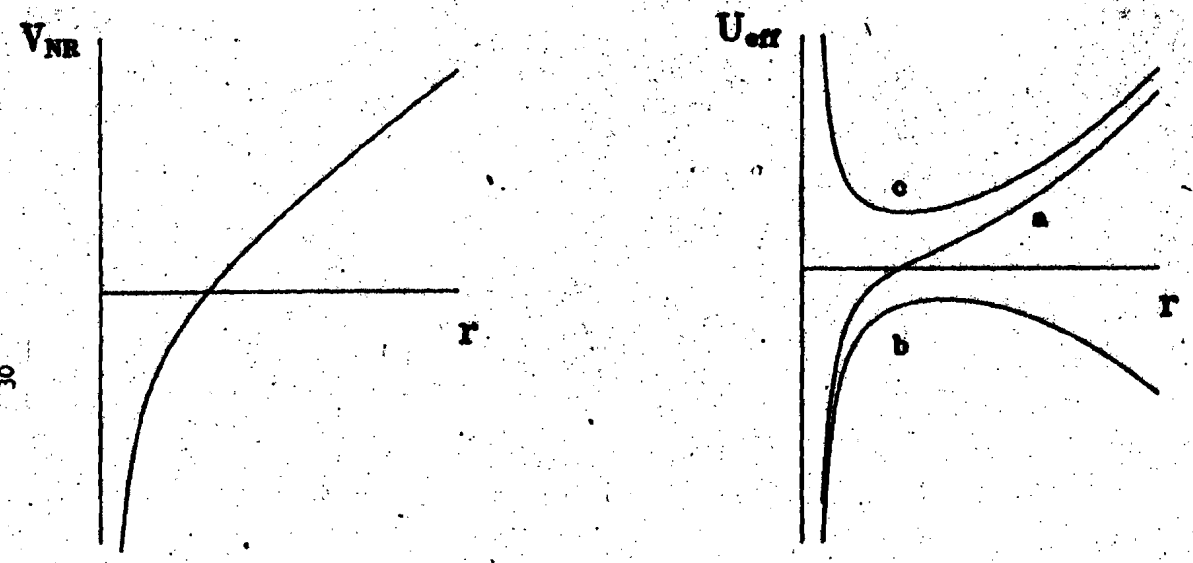

Fig. 4. Nonrelativistic potential $V_{NR}(r)$ and effective potential $U_{eff}(r)$ for different Lorenz structures of interaction. The curves (a) – (c) correspond to three choices in Sect. 4.

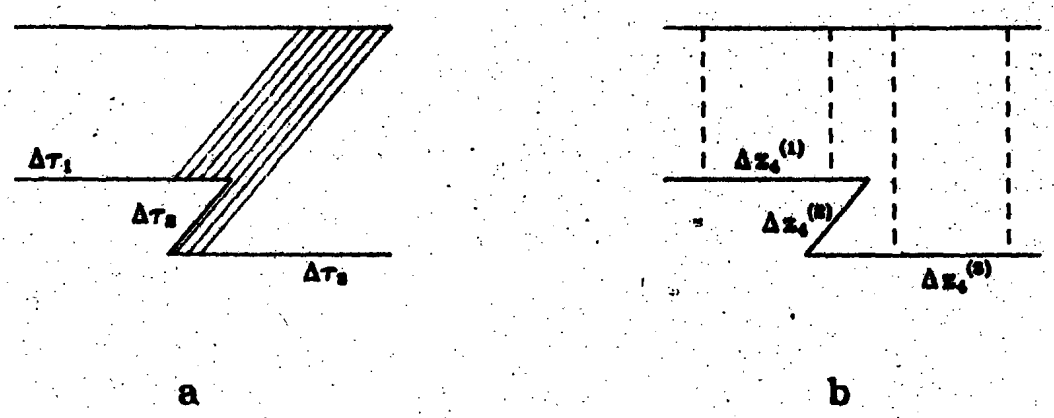

Fig. 3. The trajectory corresponding to virtual pair creation: a)scalar case, b) vector case.

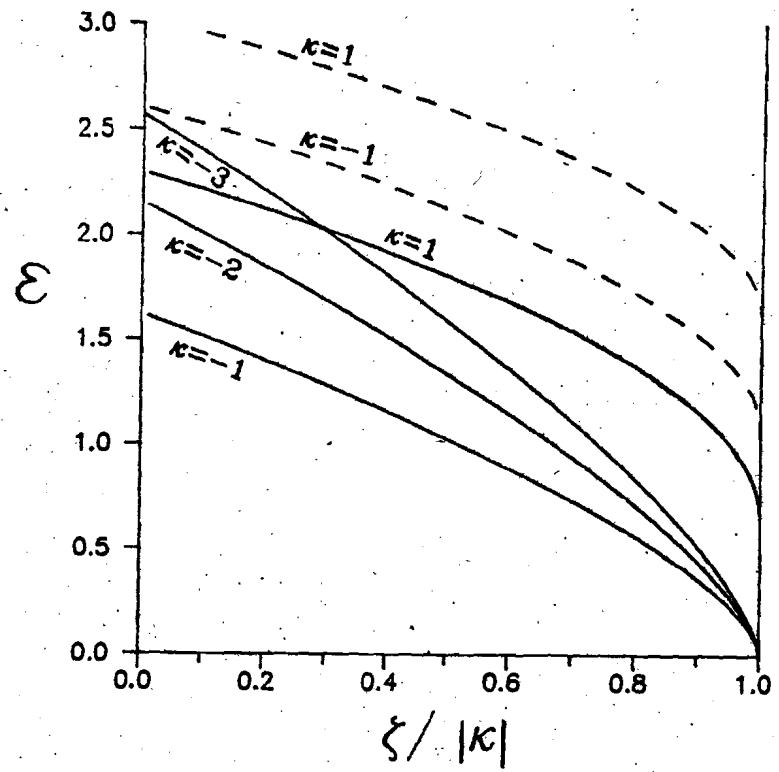

Fig. 5. The energy spectrum for the Dirac equation with potential (26). The solid curves correspond to the $n = 1$ states, the dashed ones – to $n = 2$. The values of κ are shown at the curves.

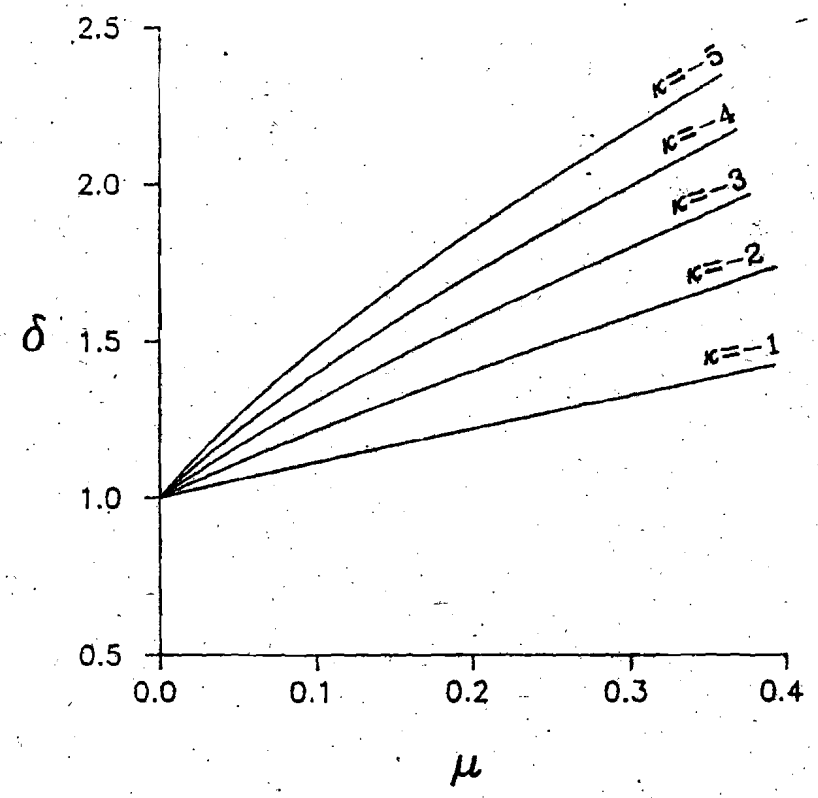

Fig. 6. The behaviour of energies of the $n = 1, \kappa < 0$ states near $\zeta = |\kappa|$. Here $\mu = (1 - \zeta^2/\kappa^2)^{1/2}$ and $\delta = \pi^{1/2}\varepsilon/\mu$.

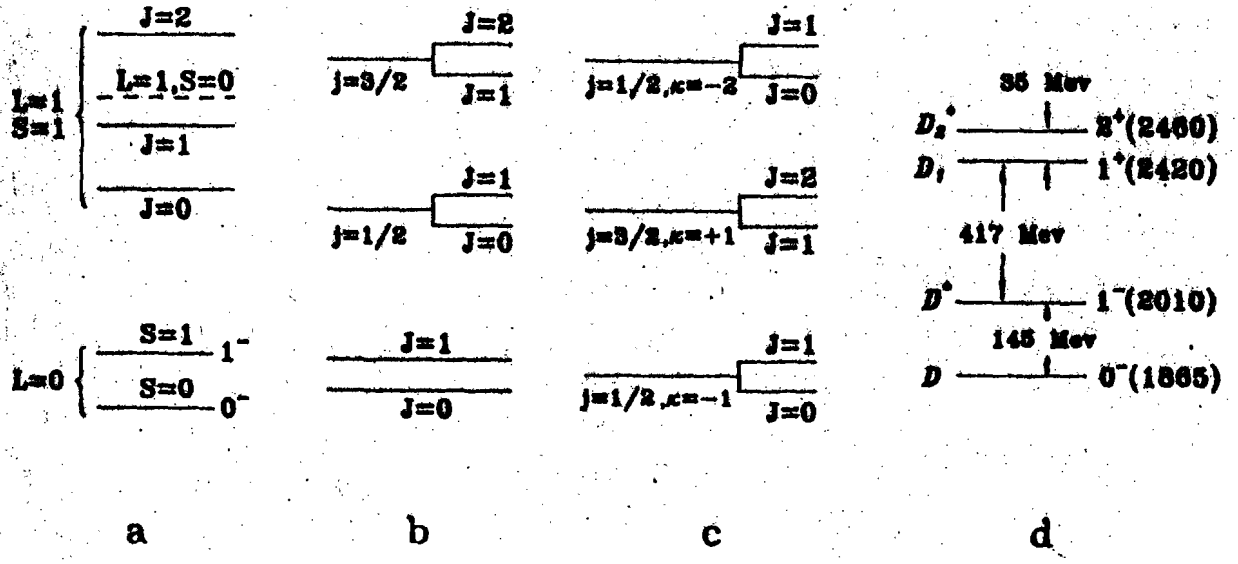

Fig. 7. The energy spectrum for the heavy quark–light antiquark system (qualitatively):
(a) $m_1, m_2 \gg M = \sigma^{1/2}$; (b) $m_1 \sim M, m_2 \gg M$;
(c) $m_1 \to 0, m_2 \to \infty$; (d) experiment.
Note that energy scale in Fig. (a) is strongly enlarged as compared to Figs. (b)–(d).

References

[1] B.Grinstein // preprint HUTP-91/A029; J.D.Bjorken // preprint SLAC-PUB-5278.

[2] Yu.A.Simonov // Nucl.Phys. B324 (1989) 67; M.Schiestl and H.G.Dosch // Phys.Lett. B209 (1988) 85.

[3] D.Gromes // preprint HD-THEP-87-21.

[4] W.Lucha, F.Schöberl and D.Gromes // Phys.Rep. 200 (1991) 127.

[5] M.Igar and M.Wise // Phys.Lett. B232 (1989) 113; B237 (1990) 527.

[6] H.G.Dosch and Yu.A.Simonov // Phys.Lett. B205 (1988) 339; H.G.Dosch // Phys.Lett. B190 (1987) 177.

[7] Yu.A.Simonov // Nucl. Phys. B307 (1988) 512.

[8] Yu.A.Simonov // Yad. Fiz. 54 (1991) 192.

[9] I.Pomeranschuk and Ya.Smorodinsky // J. of Phys USSR 9 (1945) 315.

[10] Ya.B.Zel'dovich and V.S.Popov // Uspekhi Fiz. Nauk 105 (1971) 403.

[11] W.Greiner, B.Müller and J.Rafelski: Quantum Electrodynamics of Strong Fields, Springer-Verlag, Heidelberg, 1985.

[12] Yu.A.Simonov // Z.Phys. C53 (1992) 419.

[13] Yu.A.Simonov // preprint ITEP 97-89 (1989).

[14] A.M.Polyakov // Nucl.Phys. B164 (1980) 171. V.S.Dotsenko and S.N.Vergeles // Nucl.Phys. 169 (1980) 527. R.A.Brandt et al. // Phys.Rev. D26 (1982) 3611.

[15] Yu.A.Simonov and J.A.Tjon // preprint Utrecht Univ., 1992.

[16] V.Marquard and H.G.Dosch // Phys.Rev. D36 (1987) 2236.

[17] M.Shifman, A.Vainshtein and V.Zakharov // Nucl.Phys. B147 (1979) 385, 448.

[18] M.Campostrini, A.Di Giacomo and G.Mussardo // Z.Phys. C25 (1984) 173;
A.Di Giacomo et al. (to be published).

[19] Yu.A.Simonov // Phys.Lett. B226 (1989) 151.

[20] W.Buchmüller // Phys.Lett B112 (1982) 479;
R.D.Pisarski and J.D.Stack // preprint Fermilab PUB-86/122-T.

[21] A.I.Akhiezer and V.B.Berestetsky: Quantum Electrodynamics, 3-rd ed. Nauka, Moscow, 1969 (in Russian).

[22] L.D.Landau and E.M.Lifshitz: Quantum Mechanics, Pergamon, N.Y. 1991.

[23] K.M.Case// Phys. Rev. 80 (1950) 797.

[24] W.Pieper and W.Greiner// Z. Phys. 218(1969) 327.

[25] V.S.Popov// Pis'ma v ZhETF 11 (1970) 254;
Yad.Fiz. 12 (1970) 429.

[26] V.D.Mur and V.S.Popov// Yad. Fiz. 18 (1973) 684.

[27] V.S.Popov// Yad. Fiz. 14 (1971) 458.

[28] I.S.Gradstein and I.M.Ryzhik : Tables of Integrals, Series, and Products. Academic, N.Y., 1980.

В.Д.Мур и др.
Описание релятивистской кварк-антикварковой системы уравнениями Дирака для случая легкого кварка и тяжелого антикварка.

Подписано к печати 7.09.92 Формат 60x90 I/8 Офсетн.печ.
Усл.-печ.л.2,25. Уч.-изд.л.I,6. Тираж 260 экз. Заказ 83
Индекс 3649

Отпечатано в ИТЭФ, II7259, Москва, Б.Черемушкинская,25